

Nanostructured ZrO₂ ceramic PVD coatings on Nd-Fe-B permanent magnets

Anton Taran,¹ Igor Garkusha,¹ Valerij Taran,¹ Alexander Timoshenko,¹ Ivan Misiruk,¹ Vadym Starikov,^{2,*} Alexey Baturin,² Tamara Skoblo,³ Svetlana Romaniuk³ and Athanasios G. Mamalis^{4,*}

¹ *Institute of Plasma Physics of NSC KIPT, Kharkov, Ukraine*

² *National Technical University “Kharkov Polytechnic Institute”, Kharkov, Ukraine*

³ *National Technical University of Agriculture, Kharkov, Ukraine*

⁴ *Project Centre for Nanotechnology and Advanced Engineering, NCSR “Demokritos”, Athens, Greece*

The results of vacuum-arc deposition (PVD) of thin ZrO₂ coatings to protect the surface of Nd-Fe-B permanent magnets used as repelling devices in orthodontics are presented. Magnetic devices are offered as an optimum and biologically safe force-generating system for orthodontic tooth movement. The structure, phase composition and mechanical properties of zirconium oxide films have been investigated by means of SEM, XRD, EDX, XRF and nanoindentation methods. The coatings are formed of polycrystalline ZrO₂ films of monoclinic modification with average grain size 25 nm. The influence of the ZrO₂ coating in terms of its barrier properties for corrosion in quasiphysiological 0.9% NaCl solution has been studied. Electrochemical measurements indicated good barrier properties of the coating on specimens in the physiological solution environment.

Keywords: coating, corrosion, structure, vacuum-arc deposition, zirconium dioxide

1. Introduction

Hard magnetic alloys (permanent magnets) are used as components in a wide range of industrial applications, in regulating and measuring controls and in medical equipment. Neodymium iron boron (Nd-Fe-B) or “neo” magnets offer the highest energy comparable of any material today and are available in a wide range of shapes, sizes and grades. However, the neo magnets have some limitations due to their susceptibility to corrosion. Thus, for medical applications, a

* Corresponding authors. E-mail addresses: vadym_starikov@ukr.net; a.mamalis@inn.demokritos.gr

protective coating is highly recommended. In this case, zirconium dioxide in the form of a thin buffer layer on the magnet surface is a promising candidate, due to its biological inertness and corrosion resistance.

Nd-Fe-B magnets are frequently used as repelling devices in orthodontics and are advantageous over other materials and devices used to move teeth, such as a push coil or elastic chain.¹ Neo magnets provide a continuous force over extended periods of time for various kinds of tooth movement, without friction. The disadvantages of their application are their corrosion products, which are toxic.

Zirconium dioxide (ZrO₂) ceramics possess high resistance to crack propagation, high fracture toughness, a high thermal expansion coefficient ($\alpha = 11 \times 10^{-6} \text{ K}^{-1}$, similar to some types of steel) and, due to these properties, it is very suitable for joining ceramic and steel. It is moreover an excellent thermal insulator with a low thermal conductivity of 2.5 to 3 W/mK.²

Various deposition methods, namely thermal oxidation of zirconium films, electron beam evaporation, pulsed laser deposition, DC/RF magnetron sputtering, the sol-gel process and spray pyrolysis were employed for the preparation of ZrO₂ thin films.²⁻⁸ Physical vapour deposition (PVD) methods of coating application including vacuum arc evaporation in a reactive medium (oxygen, nitrogen) are widely used to obtain ceramic coatings with a high melting point.⁹⁻¹¹

In our experiments, thin ZrO₂ coatings were deposited using vacuum-arc evaporation with a curvilinear filter for decreasing the number of macroparticles (MPs) emitted from the plasma flow in a Bulat-type device. The structure, chemical and phase composition of the obtained ZrO₂ coatings have been investigated. Corrosion experiments were carried out in quasiphysiological 0.9% NaCl solution.

¹ M. Prasad, M. Manoj-Kumar et al., Clinical evaluation of neodymium-iron-boron (Nd₂Fe₁₄B) rare earth magnets in the treatment of midline diastemas. *J. Clin. Exp. Dent.* **8** (2016) 164–171.

² J. Gao, Y. He and D. Wang, Fabrication and high temperature oxidation resistance of ZrO₂/Al₂O₃ micro laminated coatings on stainless steel. *J. Mater. Chem. Phys.* **123** (2010) 731–736.

³ S. Venkataraj et al., Structural and optical properties of thin zirconium oxide films by reactive direct current magnetron sputtering. *J. Appl. Phys.* **92** (2002) 3599–3607.

⁴ J.W. Bae et al., Preparation of ZrO₂ dielectric layers by subsequent oxidation after Zr film deposition with negative substrate bias voltage. *J. Metals Mater. Intl* **16** (2010) 447–452.

⁵ X. Ling et al., Influence of oxygen partial pressure on the laser-induced damage resistance of ZrO₂ films in vacuum. *Vacuum* **119** (2015) 145–150.

⁶ A. Singh et al., Investigation on depth-resolved composition of electron beam-deposited ZrO₂ thin films. *J. Appl. Surf. Sci.* **419** (2017) 337–341.

⁷ W.T. Tang et al., Synthesis and characterization of HfO₂ and ZrO₂ thin films deposited by plasma-assisted reactive pulsed laser deposition at low temperature. *J. Thin Solid Films* **518** (2010) 5442–5446.

⁸ H.H. Zhang, C.Y. Ma and Q.Y. Zhang, Scaling behavior and structure transition of ZrO₂ films deposited by RF magnetron sputtering. *Vacuum* **83** (2009) 1311–1316.

⁹ T.S. Skoblo, S.P. Romaniuk, A.I. Sidashenko, I.E. Garkusha, A.V. Taran et al., Strengthening method for thin-walled knives with multi-layer nanocoatings and quality assessment by non-destructive method. *J. Adv. Microsc. Res.* **13** (2018) 333–338.

¹⁰ A.V. Taran, I.E. Garkusha, V.S. Taran et al., Structure of biocompatible nanocoatings obtained by physical vapor deposition on flexible polyurethane for medical applications. *J. Adv. Microsc. Res.* **13** (2018) 313–319.

¹¹ V. Tereshin, V. Taran et al., Coating deposition and surface modification under combined plasma processing. *Vacuum* **73** (2004) 555–560.

2. Experimental

The ZrO_2 coatings on Nd-Fe-B magnets (Fig.1) were obtained in a Bulat-type device by a condensing vacuum-arc plasma kept free from macroparticulates by means of a curvilinear filter.¹²

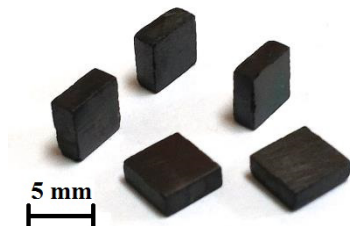


Figure 1. General view of the Nd-Fe-B magnets.

The scheme of the experimental setup is shown in Fig. 2. The filtered vacuum-arc plasma source consists of cathode 1, anode 2 and duct 4; all are surrounded by electromagnetic coils 3. The anode 2 and duct 4 are of such length and cross section that the surface of the cathode 1 is out of the line of sight from the duct outlet.

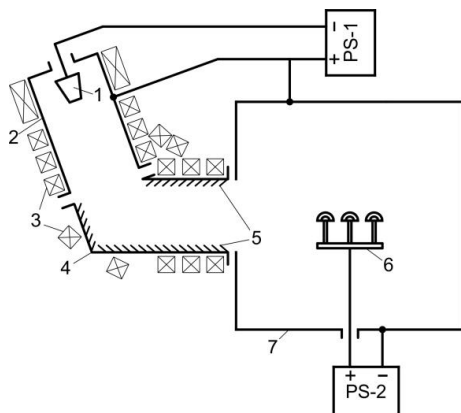


Figure 2. Scheme of the experimental equipment. 1, cathode; 2, anode; 3, electromagnetic coils; 4, duct; 5, baffles; 6, workpieces; 7, vacuum chamber; PS-1, arc discharge power supply unit; and PS-2, source of pulsed negative bias. See also main text.

The macroparticles emitted from the cathode 1 do not reach the outlet of the duct 4 but fall into the gaps between the baffles 5, whereas the plasma stream moves along a curvilinear magnetic field generated by the electromagnetic coils 3, and condenses on the surface of workpieces 6. The cathode 1 and anode 2 of the arc plasma source are connected to the power supply unit PS-1. The PS-2 is the source of the pulsed negative biasing supplied to the sample holder.

¹² V. Gasilin, O. Shvets, V. Taran et al., Filtered arc plasma discharge for coatings deposition under HF biasing of samples. *J. Inst. Appl. Plasma Sci.* **13** (2005) 87–93.

The magnet was fixed in a holder that squeezes its opposite sides with a small force, as shown in Fig. 3. Chemically pure zirconium (99.999) was used as the cathode material. The chamber was preliminarily pumped down to a pressure of 6×10^{-5} Torr. The pulsed negative bias of 1000 V with frequency 50 kHz was applied to the sample holder from the source PS-2. The rotation of the holder was turned on, the vacuum arc was ignited ($I_d = 115$ A) and the four faces of the magnets were cleaned by zirconium ions in pulsed mode: cleaning for 1.5 s and a pause of 6 s; in total 15 cycles. Then the source PS-2 was turned off, the chamber was filled with oxygen to a pressure of about 4×10^{-3} Torr and zirconium dioxide was deposited during 12 min. Then the vacuum chamber was opened, the magnets were installed in the other position (Fig. 3b) and ZrO₂ was deposited on the uncoated faces for 7 min. The target thickness of the ZrO₂ coating on the faces of the magnet was 3 μ m.

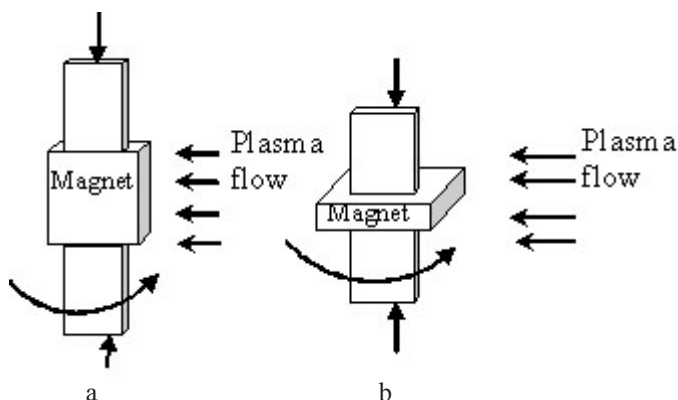


Figure 3. Experimental deposition scheme of ZrO₂ on NdFeB magnets.

The surface topography of the ZrO₂ was studied using a JEOL JSM-6390LV scanning electron microscope (SEM) with an accelerating voltage of 20 kV, while its chemical composition was examined using energy-dispersive X-ray analysis (EDX).

An energy-dispersive spectrometer SPRUT-K (AO Ukrrentgen, Ukraine) was used for X-ray fluorescence (XRF) analysis, equipped with a Si (Li) X-100 detector (Amptek, USA) in the arrangement with Si and KCl secondary targets. X-ray tube BS-22 with a shooting-through type Ag anode was used. The tube regime was: $U = 35$ kV, $I = 250$ mA; and exposure time 300 s. Film thickness was determined by XRF examination and was ~ 3 μ m.

X-ray diffraction (XRD) analysis were performed using a DRON-3M device, with Cu-K α radiation, monochromated by (002) HOPG in the diffracted beam. The XRD line scans were performed in θ - 2θ scanning mode, wherein the incident angle θ and diffracted angle 2θ are scanned simultaneously.

Nanohardness was measured using a G200 Nanoindenter (USA). The loading and unloading rates of the nanoindentation were 10 mN/min. Samples were tested to a depth of 500 nm. 6 indentations were made for each sample and the distance between them was 15 μ m.

Finally, the ZrO₂ films were analysed for their corrosion properties in 0.9% NaCl (quasiphsiological) aqueous solution.

3. Results and discussion

3.1 Composition and structure

Energy dispersive X-ray analysis (EDX) and X-ray diffraction analysis (XRD) were used to determine the chemical and phase composition of the deposited films. The EDX spectrum of the as-deposited ZrO₂ films formed at an oxygen partial pressure of 4.5×10^{-3} Torr is shown in Fig. 4a.

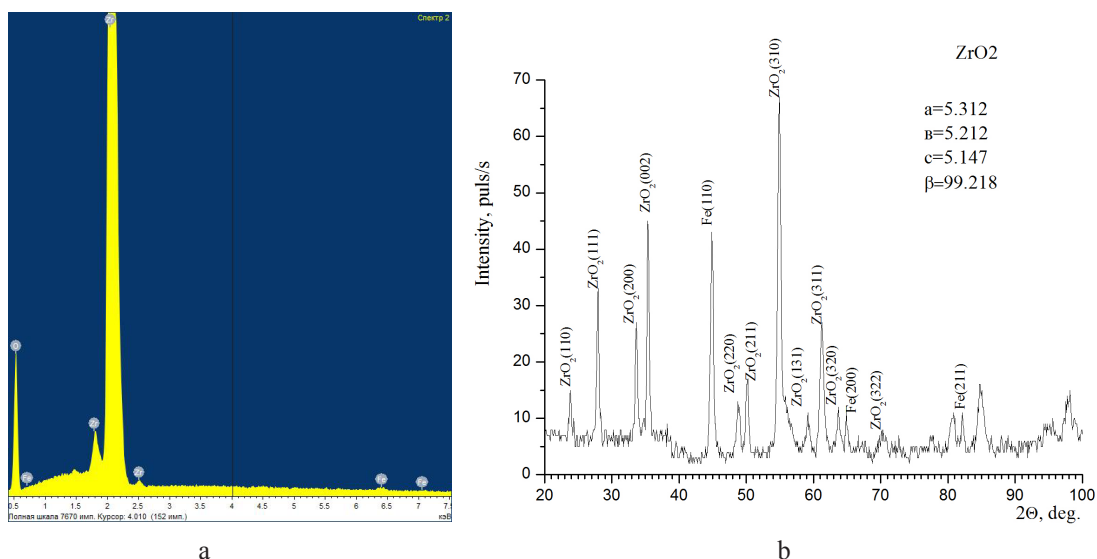


Figure 4. Zirconium oxide film: (a) EDX spectrum; (b) XRD pattern.

The EDX spectrum consisted of the characteristic zirconium and oxygen peaks without the presence of any other (impurity) peaks. The chemical composition was Zr = 30.46 atom% and O = 69.54 atom% (Table 1). It indicates that the deposited films were stoichiometric. There was no variation of the chemical composition within the film's volume.

Table 1. Chemical composition of the zirconium oxide film from EDX.

Element	Intensity	wt%	atom%
O	0.6336	28.59	69.54
Zr	0.9100	71.41	30.46

The main diffraction peaks at 26.7°, 50°, 56.9° and 61.5° relate to the (111), (211), (310) and (311) planes and reflect the monoclinic phase of ZrO₂ (Fig. 4b). The film is crystalline and exists in the single monoclinic ZrO₂ phase according to the JCPDF manual (file 37-1484), with lattice parameters $a = 5.312$, $b = 5.212$ and $c = 5.147$.

These results correlate well with literature data indicating that at low temperatures the most stable ZrO₂ phase is monoclinic, which occurs naturally as the mineral baddeleyite.¹³ At a

¹³ A. Kuwabara, T. Tohei, T. Yamamoto and I. Tanaka, *Ab initio* lattice dynamics and phase transformations of ZrO₂. *J. Phys. Rev. B* **71** (2005) 1–7.

temperature of 1478 K and ambient pressure the tetragonal structure becomes thermodynamically stable. At 2650 K the tetragonal structure changes into the cubic calcium fluoride structure (Fig. 5).

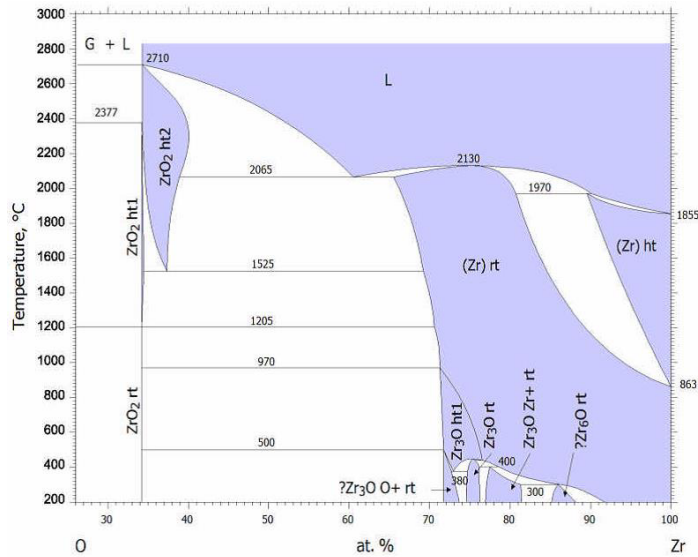


Figure 5. Zr–O phase diagram.

The crystallite size of the coatings was calculated from the full-width-at-half-maximum (FWHM) intensity (β) of the X-ray diffraction angle (θ) of the peak and the wavelength (λ) of the copper X-ray radiation using the Debye–Scherrer relation,¹⁴ assuming that no strains were developed in the coatings:

$$D = K\lambda / \beta \cos\theta \quad (1)$$

where K is a X-ray radiation-dependent constant ($K = 0.9$ for Cu– $C\alpha$) and θ is the diffraction angle. The crystallite size of the zirconium oxide film deduced was 25 nm.

The surface morphology of the deposited ZrO₂ thin film as investigated by scanning electron microscopy was homogeneous and crack-free (Fig. 6).

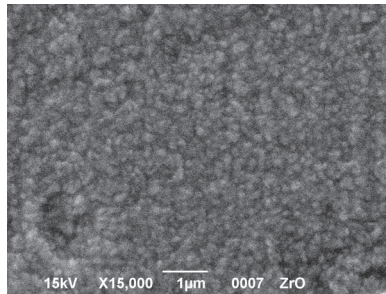


Figure 6. SEM image of the ZrO₂ coating.

¹⁴ D.B. Cullity, *Elements of X-ray Diffraction*, 2nd edn. Addison Wesley (1978).

3.2 Mechanical properties

The plasticity index H/E and the ratio H^3/E^{*2} (where $E^* = E/(1 - \mu^2)$ —the effective elastic modulus—and μ is Poisson’s ratio) are qualitative comparative characteristics of plastic deformation resistance. The shear modulus G and yield stress σ_T are defined as

$$G = E/2 \times (1 + \mu) \tag{2}$$

and

$$\sigma_T = H\mu/3. \tag{3}$$

The nanoindentation diagrams for the coating are presented in Fig. 7. H and E results for 6 indentations, as well as the G , σ_T and H^3/E^{*2} parameters, are summarized in Table 2.

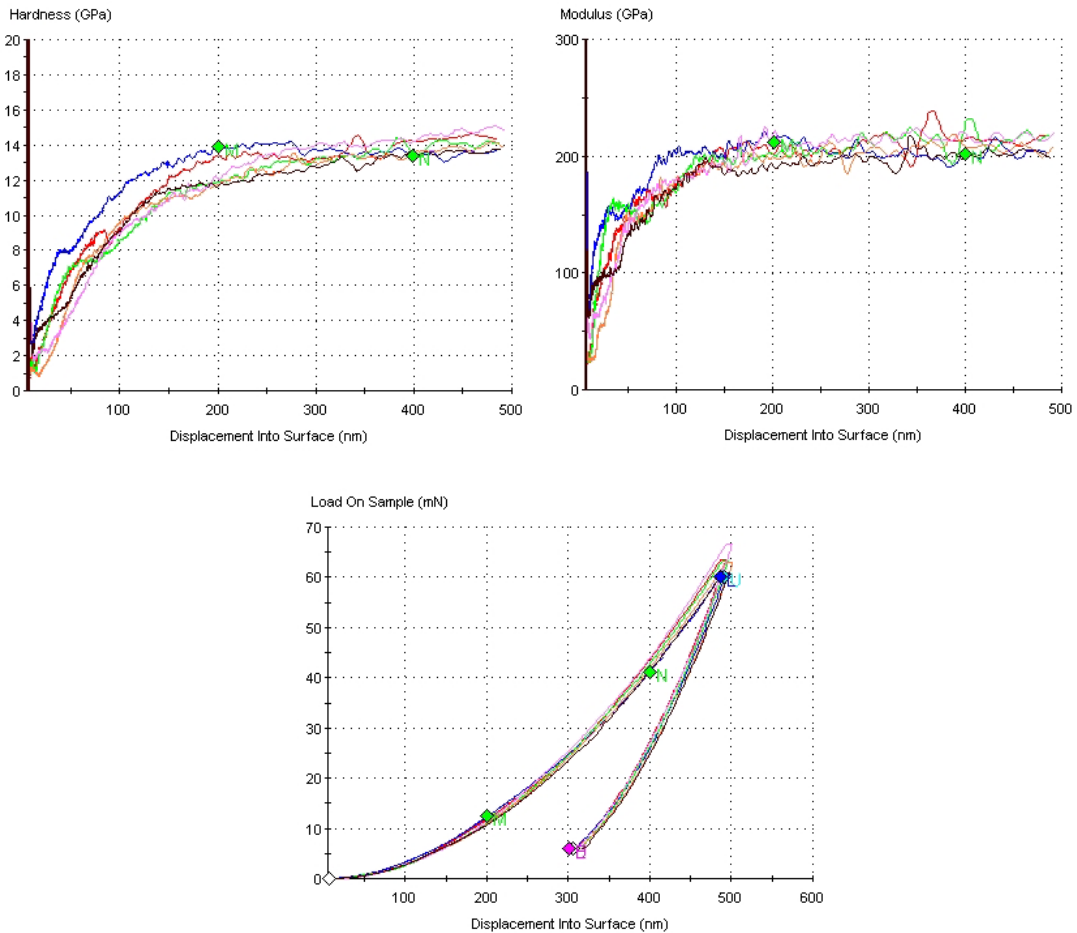


Figure 7. Nanoindentation diagrams of the zirconium oxide coating.

Table 2. Mechanical test results.

Test	E / GPa	H / GPa	H/E	H^3/E^*2	G / GPa	σ_T / MPa
1	210.32	13.49	0.064			
2	204.75	13.79	0.067			
3	208.55	12.98	0.062			
4	202.98	12.82	0.063			
5	213.96	13.56	0.063			
6	197.20	12.57	0.063			
Average	206.295	13.2	0.063	0.52	91.28	440

3.3 Corrosion properties

The electrode potential of an uncoated Nd-Fe-B magnet was $E = -0.7$ V (Fig. 8, curve 1). The deposition of a zirconia film leads to significant passivation of the magnet surface, manifested by the increase of electrode potential to $+0.01$ V (Fig. 8, curve 2). The resulting film has a high degree of continuity even at the edges and corners of the magnet. The oxide was also free from pores that could be easily detected by electrochemical testing.

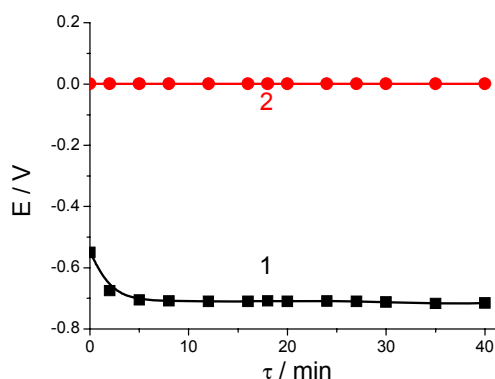


Figure 8. Electrode potentials of a Nd-Fe-B magnet in (1) the initial state and (2) with a ZrO_2 coating.

4. Summarizing conclusions

1. Monoclinic $m-ZrO_2$ thin films have been synthesized on the surface of Nd-Fe-B magnets using vacuum-arc deposition with a curvilinear filter in the presence of an oxygen plasma in a Bulat-type device.
2. SEM investigations revealed a uniform and crack-free structure of the film. XRD data revealed the formation of fine-crystalline structured films with grain size of ~ 25 nm.
3. Corrosion experiments carried out in quasiphysiological 0.9% NaCl solution showed significant passivation of the surface of the magnet, with the initially negative electrode potential E transformed into positive values. This indicates an increase of substrate resistance against electrochemical corrosion.
4. The proposed technology can be useful for applying buffer ZrO_2 coatings on NdFeB magnets used as repelling devices in orthodontics.